You might find this additional information useful...

This article cites 25 articles, 15 of which you can access free at:
http://ajpheart.physiology.org/cgi/content/full/298/1/H194#BIBL

Updated information and services including high-resolution figures, can be found at:
http://ajpheart.physiology.org/cgi/content/full/298/1/H194

Additional material and information about *AJP - Heart and Circulatory Physiology* can be found at:
http://www.the-aps.org/publications/ajpheart

This information is current as of December 18, 2009 .

Thiol-metabolizing proteins and endothelial redox state: differential modulation of eNOS and biopterin pathways

Toru Sugiyama and Thomas Michel

Cardiovascular Division, Department of Medicine, Brigham and Women's Hospital, Harvard Medical School, Boston, Massachusetts

Sugiyama T, Michel T. Thiol-metabolizing proteins and endothelial redox state: differential modulation of eNOS and biopterin pathways. *Am J Physiol Heart Circ Physiol* 298: H194–H201, 2010. First published November 6, 2009; doi:10.1152/ajpheart.00767.2009.—The intracellular redox state is stringently maintained by thiol-based antioxidants to establish a balance for the physiological and pathophysiological roles of reactive oxygen species. The relative contributions of the thioredoxin (Trx) and glutathione/glutaredoxin systems to intracellular redox balance are incompletely understood, as are the consequences of altered thiol metabolism on endothelial nitric oxide (NO) synthase (eNOS) and NO-dependent pathways in the endothelium. We designed duplex small interfering RNA (siRNA) constructs to specifically "knock down" the expression of three key thiol-metabolizing enzymes in cultured aortic endothelial cells. Transfection of siRNA constructs targeting glutathione reductase (GR), cytosolic Trx reductase (TrxR1), or mitochondrial Trx reductase (TrxR2) significantly decreased the intracellular reduced glutathione-to-oxidized glutathione ratio. siRNA-mediated knockdown of either GR, TrxR1, or TrxR2 markedly suppressed VEGF-induced NO production (measured by an electrochemical NO sensor) and also blocked eNOS enzyme activity (using the $[^3H]$arginine/$[^3H]$citrulline assay). Pretreatment of endothelial cells with *N,N'*-bis(2-chloroethyl)-*N*-nitrosourea, an inhibitor of GR and TrxR, significantly decreased VEGF-induced NO production. siRNA-mediated TrxR2 knockdown led to a marked increase in hydrogen peroxide (H_2O_2) production in endothelial cells. In contrast, knockdown of GR or TrxR1 only slightly increased H_2O_2 production. Supplementation of endothelial cells with tetrahydrobiopterin prevented the increase in H_2O_2 generation seen with siRNA-mediated knockdown of GR. These studies show that the differential regulation of thiol-metabolizing proteins leads to critical changes in oxidative and nitrosative stress pathways. Greater understanding of the differential regulation of thiol-metabolizing proteins may lead to the development of new pharmacological targets for diseases associated with oxidative stress in the vascular wall.

oxidative stress; endothelial function; thioredoxin; glutathione; nitric oxide; tetrahydrobiopterin

REACTIVE OXYGEN SPECIES (ROS) are formed as normal products of aerobic metabolism from a variety of intracellular pathways and proteins, including mitochondrial electron transport, nitric oxide (NO) synthases, NADPH oxidases, and xanthine oxidase. A fine balance between oxidizing and reducing conditions must be maintained for the normal function and survival of cells. Many vascular disease states are characterized by elevated levels of ROS: in diabetes, hypertension, or hyperlipidemia, excessive quantities of ROS lead to pathological oxidant stresses on the cellular environment. To maintain intracellular redox balance, several interrelated enzymatic systems metabolize ROS (14, 16). The roles and interactions of these diverse ROS-metabolizing pathways are incompletely understood.

A family of thiol-disulfide oxidoreductases, which includes thioredoxin (Trx) and glutaredoxin (Grx), maintains the intracellular thiol redox state and thereby modulates metabolic, signaling, and cell survival pathways (11, 25). Trx and Grx catalyze the reversible reduction of disulfides, utilizing both cysteinyl residues in their Cys-X-X-Cys active sites, reducing the target disulfide to form a mixed disulfide intermediate, which, in turn, is reduced by the active site thiolate. Under oxidizing conditions, oxidized protein thiols can form intra- and intermolecular disulfides that can subsequently be reduced by Trx or Grx. Oxidized Trx is reduced by Trx reductase (TrxR) using electrons from NADPH. In contrast to the TrxR/Trx/NADPH pathway, oxidized Grx is reduced by reduced glutathione (GSH), and the oxidized glutathione (GSSG) is subsequently recycled by glutathione reductase (GR) at the expense of NADPH. The Grx system consists of the glutathione redox couple (GSH/GSSG), GR, and Grx. Under oxidative stress conditions, in which the concentration of GSH is decreased and GSSG is increased, Grx is more likely to be oxidized (1). The GSH-to-GSSG ratio (GSH/GSSG) in the cell is an important marker of the redox environment and the major determinant of the cellular redox potential. Under normal conditions, the concentration of GSH, which is typically in the millimolar range, far exceeds the concentration of oxidized GSSG. However, the relative contributions of the Trx and GSH/Grx systems to intracellular redox balance remain incompletely understood.

Endothelial cells are importantly affected by intracellular redox state, and oxidative stress has been implicated in a broad range of cardiovascular disease states (16, 21). The endothelium plays a central role in maintaining cardiovascular homeostasis and produces a variety of redox-sensitive mediators (5, 6, 15), including NO released by the endothelial isoform of NO synthase (eNOS). NO plays a central role in control of vascular tone and platelet aggregation and has been implicated in a broad range of other cellular responses and (patho)physiological processes. The mechanisms whereby oxidative stress contributes to the development of endothelial dysfunction are complex and include effects of ROS on the biotransformations of NO and on the metabolism of eNOS cofactors, including tetrahydrobiopterin (2, 10). In vascular disease states, such as diabetes, endothelial dysfunction is characterized by a decrease in NO bioactivity and by a concomitant increase in superoxide formation, while eNOS mRNA and protein levels are maintained or even increased. "Uncoupled" eNOS generates ROS, shifting the nitroso-redox balance and having adverse conse-

Address for reprint requests and other correspondence: T. Michel, Cardiovascular Division, Brigham and Women's Hospital, Harvard Medical School, 75 Francis St., Thorn Bldg., Rm. 1210A, Boston, MA 02115 (e-mail: thomas_michel@harvard.edu).

quences in the vascular wall (4, 7, 17, 22, 24). We have recently reported that the simple depletion of tetrahydro-L-biopterin (BH4) is not sufficient to promote endothelial dysfunction, but rather that it is the concentration of intracellular oxidized biopterin (BH2), as well as the relative concentrations of BH4 and BH2, that together play a determining role in the redox regulation of eNOS-modulated endothelial responses (20). Several enzymes expressed in vascular tissues contribute to the production and efficient degradation of ROS, and an enhanced activity of oxidant enzymes and/or reduced activity of antioxidant enzymes may lead to increases in oxidative stress (14). Diverse agonists, pathological conditions, and therapeutic interventions lead to changes in the expression and activity of oxidant and antioxidant enzymes. For example, the compound N,N'-bis(2-chloroethyl)-N-nitrosourea (BCNU) is an inhibitor of TrxR and GR that is associated with endothelial dysfunction (11). However, the relationship between intracellular thiol redox state, eNOS regulation, and NO bioavailability remains incompletely understood.

The present studies use small interfering RNA (siRNA) approaches to knock down the expression of three key thiol-disulfide oxidoreductases: GR, cytosolic TrxR (TrxR1), and mitochondrial TrxR (TrxR2). Our experiments reveal differential roles of these critical thiol-metabolizing enzymes in the modulation of eNOS pathways and ROS production in cultured endothelial cells.

MATERIALS AND METHODS

Materials. Fetal bovine serum (FBS) was from HyClone Laboratories (Logan, UT). Lipofectamine 2000, Amplex Red reagent, and most cell culture reagents were from Invitrogen. Polyclonal antibodies against phospho-Akt (Ser473), Akt, and phospho-eNOS (Ser1179) were from Cell Signaling Technology (Danvers, MA). Polyclonal antibody against phospho-Ser116-eNOS was from Upstate Biotechnology (Lake Placid, NY). Monoclonal antibody against eNOS was from BD Transduction Laboratories (Lexington, KY). Polyclonal antibody against GR was from Santa Cruz Biotechnology (Santa Cruz, CA). Polyclonal antibodies against TrxR1 and TrxR2 were from Abcam (Cambridge, MA). The SuperSignal chemiluminescence detection reagents and secondary antibodies conjugated with horseradish peroxidase were from Pierce Biotechnology (Rockford, IL). BH4 and L-biopterin were from Cayman Chemical (Ann Arbor, MI). VEGF and GSH/GSSG assay kit were from Calbiochem (Darmstadt, Germany). Protein concentrations were determined using protein assay kits from Bio-Rad Laboratories (Philadelphia, PA). Determinations of protein abundance using immunoblot analyses were quantitated using a ChemiImager HD4000 (AlphaInnotech, San Leandro, CA). All other reagents were from Sigma.

Culture and treatment of cells. Bovine aortic endothelial cells (BAEC) were obtained from Cambrex (Walkersville, MD) and maintained in culture on gelatin-coated 100-mm culture dishes with Dulbecco's modified Eagle's medium supplemented with FBS (10% vol/vol), as described previously (20). BAEC are used for experiments between *passages 6* and *8* and are serum starved overnight before experiments. Treatments with VEGF and preparation of cell lysates were performed as described previously (20), with corresponding vehicle treatments as controls.

siRNA preparation and transfection. Using approaches that we pursued previously to target a broad range of endothelial cell signaling pathways (20), we designed a siRNA duplex construct targeting bovine GR mRNA (GR siRNA, sequence 5'-CUAACGUAAAAG-GUGUCUA-3', corresponding to bases 1085–1103 from the open-reading frame of the bovine GR mRNA; GenBank accession number XM_001788680.1), a siRNA targeting bovine TrxR1 mRNA (se-

quence 5'-GGCAGAUGUACACCUGAAA-3', corresponding to bases 2424–2442 from the open-reading frame of the bovine TrxR1 mRNA; GenBank accession number NM_174625.3), and a siRNA targeting bovine TrxR2 mRNA (sequence 5'-CCGCAAGUCU-GAAUUUGGA-3', corresponding to bases 941–959 from the open-reading frame of the bovine TrxR2 mRNA; GenBank accession number NM_174626.2). The duplex siRNA targeting eNOS has been previously described (20). The siRNA duplex oligonucleotides were from Ambion (Austin, TX). The nonspecific control siRNA 5'-AUUGUAUGCGAUCGCAGAC-dTdT-3' was from Dharmacon (Lafayette, CO). We found that optimal conditions for siRNA knockdown involved transfecting BAEC when cells were at 50–70% confluence, and transfected cells were maintained in Dulbecco's modified Eagle's medium/10% FBS; transfections with siRNA (45 nM) used LipofectAMINE 2000 (0.15% vol/vol) followed protocols provided by the manufacturer (Invitrogen). Fresh medium was added 5 h after transfection, and experiments are typically conducted 48 h after transfection.

Intracellular GSH and GSSG assay. The GSH/GSSG was assessed using a GSH/GSSG assay kit (Calbiochem, Darmstadt, Germany) based on the enzymatic recycling method with GR (9). The cells were harvested and the whole cell extract was prepared according to the manufacturer's instructions. The contents of GSH and GSSG were photometrically determined using a microplate reader at 412 nm, and the GSH/GSSG was calculated.

Measurement of intracellular levels of biopterins. Oxidized and reduced forms of biopterins were analyzed by the differential oxidation method of Fukushima and Nixon (8). The whole procedure was performed in the dark. BAEC were washed and suspended in cold extraction buffer (0.1 M phosphoric acid, 5 mM DTT), and protein concentrations were measured using the Bio-Rad protein assay. Proteins were removed by adding 35 μl of 2 M trichloroacetic acid (TCA) to 300 μl of the extracts, followed by centrifugation. To determine total biopterins [reduced (BH4) plus oxidized (BH2) biopterin] by acid oxidation, 100 μl of cell extract were mixed with 15 μl of 0.2 M TCA and 15 μl of 1% iodine in 2% KI in 0.2 M TCA. To determine BH2 and biopterin by alkali oxidation, 15 μl of 1 M NaOH were added to 100 μl of extract, followed by addition of 15 μl of 1% iodine/2% KI in 3 M NaOH. After incubation at room temperature for 1 h in the dark, excess iodine was reduced by adding 25 μl of fresh ascorbic acid (20 mg/ml). After centrifugation, 10 μl of supernatant were injected into a HPLC system (Agilent 1100 series; Agilent Technologies, Palo Alto, CA) equipped with a 150 × 0.32-mm ODS Hypersil column (Thermo Scientific, Waltham, MA), and coupled to a helium-cadmium laser-induced highly sensitive fluorescent detector (325 nm laser, series 56; Melles Griot, Carlsbad, CA; ZETALIF detector, model LIF-SA-03; Picometrics, Ramonville, France), as we have previously described (20). The mobile phase was methanol-doubly distilled H_2O (5:95 vol/vol) with a flow rate of 400 μl/min that was reduced to 4 μl/min with a precolumn flow splitter (100:1, series 620; Analytical Scientific Instruments, El Sobrante, CA) before laser-induced fluorescence detection. The criteria used for identification of biopterin were fluorescence and retention time compared with the standards. BH4 concentration, expressed as picomoles per milligram of protein, was calculated by subtracting BH2 + biopterin from total biopterins.

eNOS activity assay. eNOS activity was quantified as the formation of L-[³H]citrulline from L-[³H]arginine, as described before (20). Briefly, the reactions are initiated by adding L-[³H]arginine (10 μCi/ml, diluted with unlabeled L-arginine to give a final concentration of 10 μM) plus various drug treatments; each treatment was performed in triplicate cultures, which were analyzed in duplicate.

Electrochemical measurement of NO. NO production from cells (as extracellular nitrite) was measured by using an NO electrode sensor system (BioStat, ESA, Chelmsford, MA). Cell culture medium was replaced with Dulbecco's phosphate-buffered saline, and various drugs were added as indicated. After incubation for varying times,

aliquots were removed and added to the reagent solution (100 mM H_2SO_4, 100 mM NaI) to generate NO from the NO_2 present in the extracellular medium; NO is then detected with the electrochemical sensor. The absolute NO_2^- concentrations were calculated against a standard curve prepared by using $NaNO_2$ solution; the redox current generated is directly proportional to the NO_2^- concentration in the solution. After the experiment, the cells were harvested to determine protein concentration, permitting NO_2^- production to be reported as picomoles per milligram protein per minute.

Measurement of H_2O_2. H_2O_2 production from cells was quantitated using the Amplex Red fluorescence assay using previously described methods (18, 20). Cell culture medium was replaced with Amplex Red reaction mixture (50 μM Amplex Red, 0.1 U/ml horseradish peroxidase, and 10 U/ml superoxide, diluted in Dulbecco's phosphate-buffered saline). This method detects both superoxide and H_2O_2, since the addition of superoxide dismutase to the "conditioned" media leads to the quantitative conversion of superoxide to H_2O_2 (20). After incubation for varying times as indicated, aliquots were withdrawn, and fluorescence was quantitated using a FluoroMax-2 spectrofluorometer (JY-Spex, Edison, NJ) at an excitation wavelength of 530 nm and an emission wavelength of 590 nm. The absolute H_2O_2 concentrations were calculated against a standard curve prepared by using H_2O_2 solution. Cells were then harvested to determine protein concentration, permitting H_2O_2 production to be reported as picomoles per milligram protein per minute.

Immunoblot analysis. BAEC cell lysates were prepared using a cell lysis buffer (50 mM Tris·HCl, pH 7.4, 150 mM NaCl, 1% Nonidet
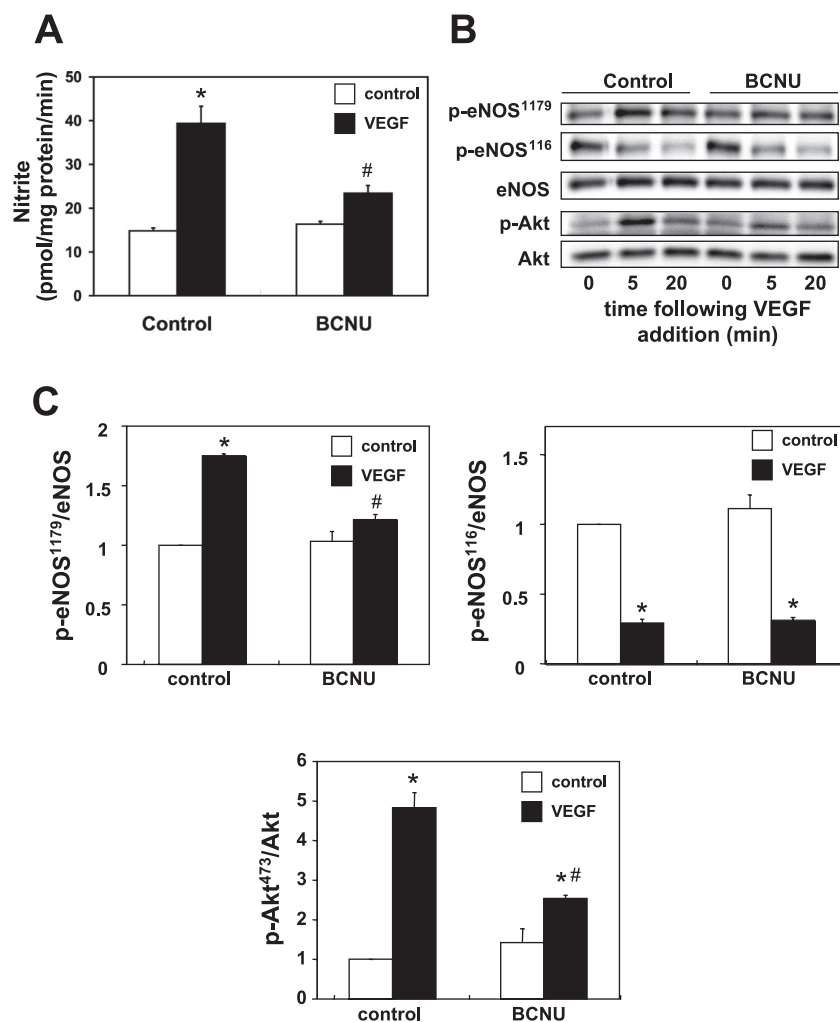
P-40, 0.025% sodium deoxycholate, 1 mM EDTA, 2 mM Na_3VO_4, 1 mM NaF, 2 μg/ml leupeptin, 2 μg/ml antipain, 2 μg/ml soybean trypsin inhibitor, and 2 μg/ml lima trypsin inhibitor). Immunoblot analyses of endothelial protein expression and phosphorylation were assessed as described previously in detail (13). Quantitative densitometric analyses of immunoblots were performed using a ChemiImager HD4000 (AlphaInnotech).

Statistical analysis. All experiments were performed at least three times. Mean values for individual experiments are presented as means $\pm$ SE. Statistical differences were assessed by ANOVA or *t*-test when appropriate. A *P* value of <0.05 was considered significant.

RESULTS

Effects of the GR/TrxR inhibitor BCNU on eNOS. We first investigated the effects of the GR/TrxR inhibitor BCNU on NO production and phosphorylation of eNOS and Akt in BAEC. As shown in Fig. 1*A*, treatment of endothelial cells with BCNU significantly attenuated VEGF-induced NO production. BCNU also decreased VEGF-induced phosphorylation of kinase Akt at serine residue 473; VEGF-promoted phosphorylation of eNOS at the activating serine residue 1179 was similarly inhibited, whereas phosphorylation of eNOS at the inhibitory serine 116 was not affected (Fig. 1, *B* and *C*).

Fig. 1. Effects of the glutathione reductase (GR)/thioredoxin reductase (TrxR) inhibitor N,N′-bis(2-chloroethyl)-N-nitrosourea (BCNU) on VEGF-stimulated nitric oxide (NO) production and endothelial NO synthase (eNOS) phosphorylation in cultured endothelial cells. *A*: NO production was measured in endothelial cells treated with the GR/TrxR inhibitor BCNU (50 μM for 2 h) or with vehicle, and then incubated with VEGF or vehicle, as shown. NO was determined using an electrochemical sensor, as described in the text. *B*: immunoblots analyzed in endothelial cells treated with BCNU for 2 h, and then incubated with VEGF (20 ng/ml) for the indicated times, probed with antibodies as shown. *C*: results of densitometric analyses from pooled data, plotting the ratios of phosphorylated eNOS (p-eNOS) and Akt (p-Akt) to total eNOS and Akt, respectively, relative to the signals present in the unstimulated cells. Each value represents the mean $\pm$ SE derived from four independent experiments. *P < 0.01 for VEGF vs. control cells. #P < 0.01 for BCNU vs. control cells (determined by ANOVA).

siRNA-mediated downregulation of GR, TrxR1, and TrxR2 expression in BAEC. We designed duplex siRNA constructs to knock down the expression of GR, TrxR1, and TrxR2 in cultured endothelial cells, as described in detail in MATERIAL AND METHODS. As shown in Fig. 2, transfection of siRNA constructs targeting GR, TrxR1, or TrxR2 specifically knocked down their targeted proteins by 83 ± 4, 70 ± 4, or $88 \pm 4\%$, respectively (relative to control siRNA-treated cells; $n = 10$ for each construct, $P < 0.01$). There was no effect on the expression of several other nontargeted signaling proteins in these cells (see also Fig. 6).

Intracellular GSH/GSSG in siRNA-transfected endothelial cells. We next determined the concentrations of intracellular GSH and GSH in these transfected cells (see Table 1), which allowed us to calculate the intracellular GSH/GSSG (Fig. 3) following siRNA-mediated knockdown of GR, TrxR1, or TrxR2, and to thereby determine the effects of these knockdowns on intracellular glutathione redox state. siRNA-mediated GR knockdown markedly decreased the intracellular GSH/GSSG ($53 \pm 10\%$ decrease compared with control siRNA-transfected cells, $n = 4$, $P < 0.01$). siRNA-mediated knockdown of TrxR1 or TrxR2 knockdown decreased the intracellular GSH/GSSG by 56 ± 9 or $54 \pm 8\%$ (each $n = 4$, $P < 0.01$), respectively (Fig. 3).

Intracellular levels of BH4 and total biopterins following siRNA-mediated knockdown of GR, TrxR1, or TrxR2. We next determined the intracellular concentrations of biopterins following siRNA-mediated knockdown of GR, TrxR1, or TrxR2 to determine the effects of these knockdowns on the metabolism of BH4, a key redox-active cofactor for eNOS. siRNA-mediated knockdown of either GR or TrxR1 significantly decreased the intracellular BH4 level by 67 ± 7 or $48 \pm 20\%$ (each $n = 4$, $P < 0.05$), respectively; there was no significant change in the amount of total cellular biopterins (Fig. 4A). By contrast, siRNA-mediated TrxR2 knockdown had no significant effect on the intracellular BH4 level and total biopterins. The percentage of BH4 relative to total cellular biopterins was decreased by GR or TrxR1 knockdown (respectively showing a 51 ± 12 or $34 \pm 6\%$ decrease compared with control siRNA-treated cells; for both constructs, $n = 4$, $P < 0.05$), whereas TrxR2 knockdown had no significant effect on the BH4-to-total biopterins ratio (Fig. 4B).

Effects of siRNA-mediated GR, TrxR1, or TrxR2 knockdown on VEGF-stimulated NO production. To explore the effects of alterations of intracellular thiol redox state on eNOS activity,

we measured eNOS enzyme activity (assaying the formation of [³H]citrulline from L-[³H]arginine) and NO production (using an electrochemical NO sensor) in endothelial cells transfected with GR, TrxR1, or TrxR2 siRNA (Fig. 5). The addition of VEGF (20 ng/ml) elicited a significant increase in eNOS enzymatic activity and in NO production in control siRNA-transfected cells ($P < 0.01$). siRNA-mediated knockdown of either GR, TrxR1, or TrxR2 markedly suppressed VEGF-induced eNOS enzyme activity and also decreased NO production by 83 ± 2, 92 ± 2, or $96 \pm 2\%$, respectively (for each construct $n = 4$; $P < 0.01$ compared with control siRNA-transfected cells). Supplementation of BAEC with BH4 (10 µM), which is sufficient to restore intracellular total biopterin and BH4 levels (20), did not restore the suppression of NO production seen following siRNA-mediated knockdowns of GR, TrxR1, or TrxR2 (data not shown).

Effects of siRNA-mediated GR, TrxR1, or TrxR2 knockdown on VEGF-promoted Akt and eNOS phosphorylation. We assessed VEGF-induced Akt phosphorylation and eNOS phosphorylation/dephosphorylation in immunoblots probed using antibodies directed against eNOS phosphorylated at Ser1179; eNOS phosphorylated at Ser116; total eNOS; phospho-Akt; and total Akt. As shown in Fig. 6, siRNA-mediated knockdown of TrxR1, but not of GR or TrxR2, blocked VEGF-induced eNOS phosphorylation at Ser1179 and phosphorylation of Akt, whereas phosphorylation of eNOS at Ser116 was not affected by any of these siRNA targeting constructs.

Effects of siRNA-mediated knockdown of GR, TrxR1, or TrxR2 on endothelial cell ROS production. To investigate the effects of alterations of thiol redox state on the generation of

Table 1. *Intracellular concentrations of GSH and GSSG in siRNA-transfected endothelial cells*

siRNA	Control	GR	TrxR1	TrxR2
[GSH]	124.1 ± 4.7	136.1 ± 3.3	$152.9 \pm 9.3*$	125.2 ± 2.5
[GSSG]	0.58 ± 0.1	$1.13 \pm 0.1*$	$1.44 \pm 0.2*$	$1.13 \pm 0.1*$

Each data point represents the mean $\pm$ SE in nmol/mg protein, derived from four independent experiments, each performed in duplicate. Shown are the concentrations of GSH and GSSG in endothelial cells transfected with control, glutathione reductase (GR), cytosolic Trx reductase (TrxR1), or mitochondrial Trx reductase (TrxR2) small interfering RNA (siRNA). Forty-eight hours following siRNA transfections, the intracellular concentrations of GSH and GSSG were assessed, as detailed in the text. $*P < 0.01$ vs. control siRNA-transfected cells (ANOVA).
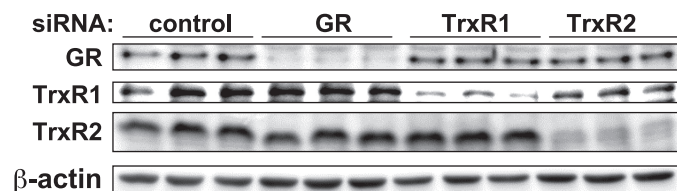

Fig. 2. Small interfering RNA (siRNA)-mediated knockdown of thiol-metabolizing proteins in cultured endothelial cells. This figure shows a representative immunoblot of cell lysates prepared from endothelial cells transfected with duplex siRNA constructs (45 nM) targeting GR, cytosolic Trx reductase (TrxR1), or mitochondrial Trx reductase (TrxR2), or a control sequence. Forty-eight hours after transfection, cells were harvested, and protein expression was analyzed in immunoblots probed with antibodies as shown. This figure is representative of five similar experiments that yielded equivalent results.
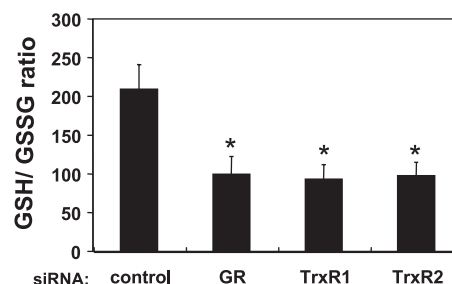

Fig. 3. Intracellular GSH-to-GSSG ratio in siRNA-transfected endothelial cells. Endothelial cells were transfected with siRNA constructs targeting GR, TrxR1, TrxR2, or a control sequence, and intracellular GSH-to-GSSG ratios were assessed as detailed in the text. Each value represents the mean $\pm$ SE derived from four independent experiments, each performed in duplicate. $*P < 0.01$, vs. control siRNA-transfected cells (ANOVA).
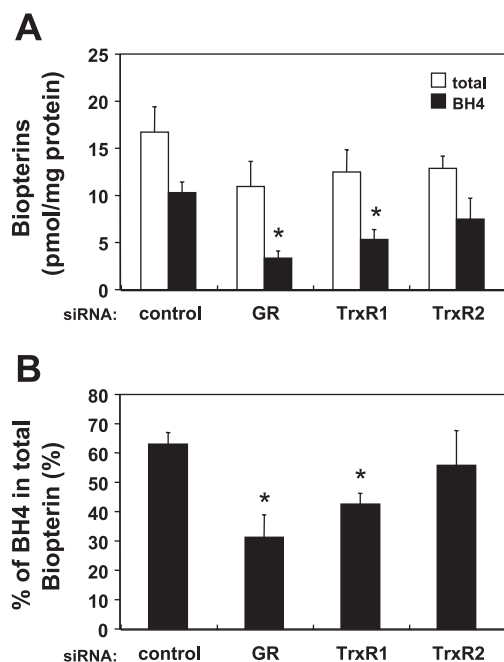
Fig. 4. Intracellular levels of reduced and total biopterins in siRNA-transfected endothelial cells. *A*: endothelial cells were transfected with siRNA constructs targeting GR, TrxR1, TrxR2, or a control sequence, and intracellular levels of tetrahydro-L-biopterin (BH4) and total biopterins were assessed by differential oxidation and HPLC. The open bars indicate the concentration of total cellular biopterins, and the solid bars indicate the concentration of reduced biopterins (BH4). *B*: fraction of intracellular BH4 relative to the total biopterins level. Each data point represents the mean $\pm$ SE derived from three independent experiments, each performed in duplicate. *$P < 0.01$, vs. control siRNA-transfected cells (ANOVA).

ROS, we measured H_2O_2 production in endothelial cells transfected with duplex siRNA constructs targeting GR, TrxR1, or TrxR2. The basal level of H_2O_2 production in different independent experiments shows a ~1.6-fold variance, as we have previously reported (20). This variance in basal H_2O_2 production probably reflects the fact that these experiments are performed in primary endothelial cells, and there is inevitably lot-to-lot variability. But within each series of independent experiments, the variance is low, and the results shown are statistically significant. Nonetheless, caution should be exercised when extrapolating these results to other cellular systems. As shown in Fig. 7*A*, siRNA-mediated knockdown of GR or TrxR1 slightly but significantly increased H_2O_2 production quantitated using the Amplex Red fluorescence assay (increases of 38 ± 4 or $32 \pm 5\%$ respectively, compared with control siRNA-transfected cells; $n = 4$, $P < 0.01$). These increases in H_2O_2 production seen with siRNA-mediated knockdown of GR or TrxR1 were abrogated by simultaneous siRNA-mediated knockdown of eNOS. In contrast to the modest effects of GR and TrxR1, TrxR2 knockdown led to a marked increase in H_2O_2 production ($89 \pm 5\%$ increase in H_2O_2 production compared with control siRNA-transfected cells, $n = 4$, $P < 0.01$); this effect was entirely unaffected by simultaneous siRNA-mediated eNOS knockdown. To explore the enzymatic sources of H_2O_2 that account for the increase in ROS seen after siRNA-mediated TrxR2 knockdown, we exploited a series of pharmacological inhibitors of ROS production. Treatment of endothelial cells with rotenone, a mitochon-

drial complex I inhibitor, or antimycin A, a mitochondrial complex III inhibitor, abrogated TrxR2 knockdown-mediated increase in H_2O_2 production (Fig. 7*B*); antimycin A treatment can increase mitochondrial production of ROS, but our analyses of extracellular H_2O_2 production failed to show an increased signal using the Amplex Red assay. Treatment of transfected endothelial cells with apocynin (NADPH oxidase inhibitor), oxypurinol (xanthine oxidase inhibitor), or N^G-nitro-L-arginine methyl ester (eNOS inhibitor), had no effect on the increase in H_2O_2 production seen following TrxR2 siRNA-mediated knockdown (Fig. 7*B*). We next examined the effects of exogenous BH4 on the H_2O_2 production. Supplementation with BH4 (10 μM) abolished the increase in H_2O_2 generation seen following siRNA-mediated knockdown of GR, whereas the increased production H_2O_2 seen with siRNA-mediated TrxR1 or TrxR2 knockdown was not suppressed by the addition of BH4 (Fig. 7*C*).

DISCUSSION

These studies have explored the roles of three critical thiol-disulfide oxidoreductases in the differential regulation of eNOS signaling pathways and H_2O_2 metabolism in cultured endothelial cells, and affirm the critical roles of ROS in the modulation of cellular responses. We found that pharmacological inhibition of GR and TrxR with BCNU decreased VEGF-induced phosphorylation of Akt and eNOS and suppressed VEGF-promoted NO production from endothelial cells (Fig. 1), consistent with previous observations (23) that implicated these thiol-metabolizing enzymes in eNOS regulation. However,
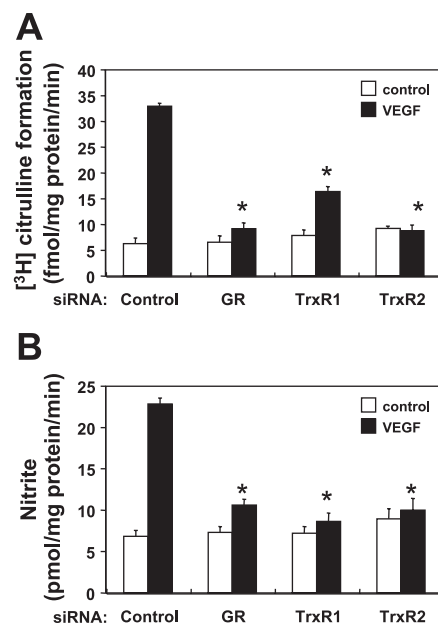

Fig. 5. Effects of siRNA-mediated knockdown of thiol-metabolizing proteins on VEGF-stimulated eNOS activity. *A*: eNOS activity was measured 48 h after transfection with siRNA targeting constructs, as shown. Endothelial cells were incubated with L-[³H]arginine, and treated with VEGF or vehicle. eNOS enzyme activity was quantitated by determining the formation of L-[³H]citrulline from L-[³H]arginine, as described in the text. *B*: NO production was assayed 48 h after transfection with siRNA targeting constructs. Endothelial cells were incubated with VEGF for 30 min, and NO_2^- levels in the media were determined using an electrochemical NO sensor, as detailed in the text. Each data point represents the mean $\pm$ SE derived from four independent experiments. *$P < 0.01$ for VEGF vs. control cells (ANOVA).
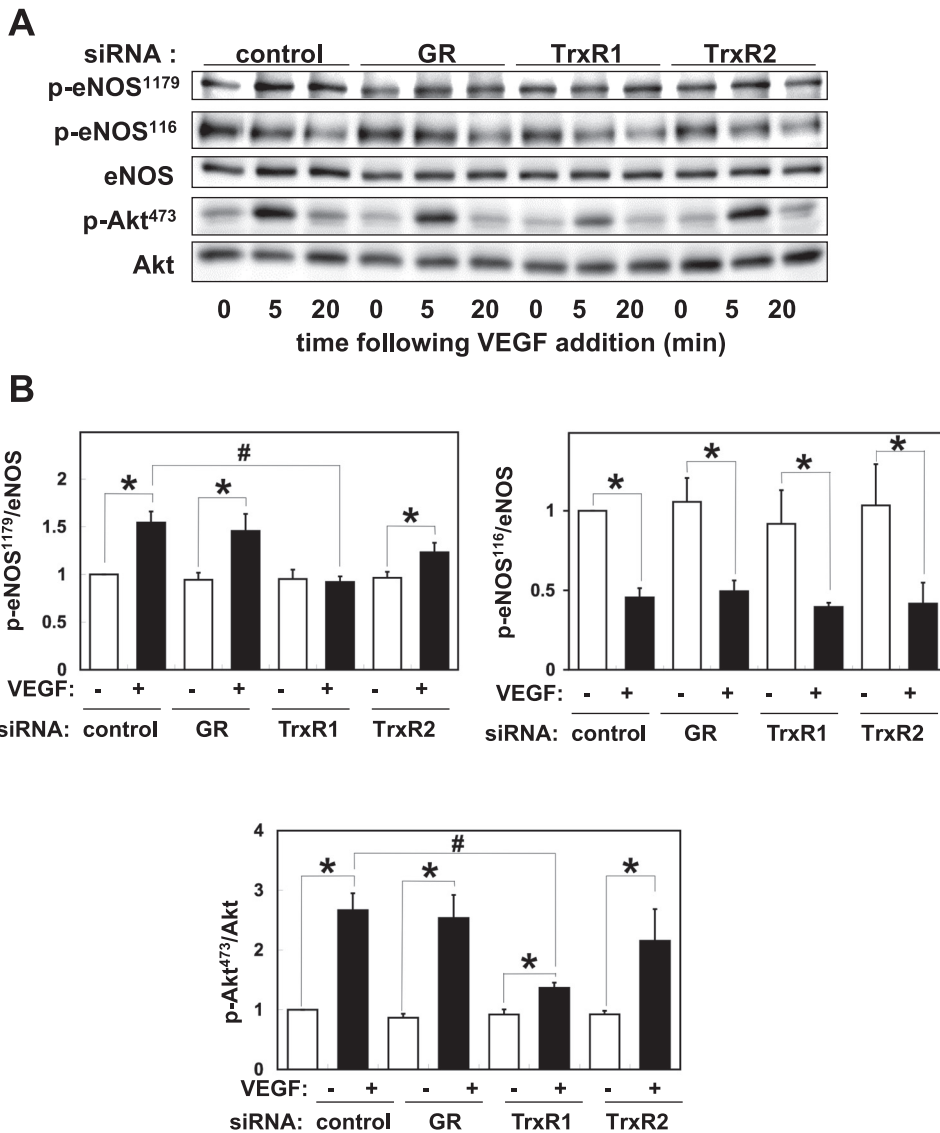
Fig. 6. eNOS signaling responses following siRNA-mediated knockdown of thiol-metabolizing proteins. *A*: immunoblots were analyzed in endothelial cell lysates prepared from bovine aortic endothelial cells (BAEC) transfected with control, GR, TrxR1, or TrxR2 siRNA targeting constructs as shown, and then treated with VEGF for the indicated times. Cell lysates were resolved by SDS-PAGE and probed in immunoblots using antibodies directed against phosphoserine[1179]-eNOS, phosphoserine[116]-eNOS, total eNOS, p-Akt, and total Akt. Shown are representative data of four independent experiments. *B*: results of densitometric analyses from pooled data, plotting the ratios of p-eNOS and p-Akt to total eNOS and Akt, respectively, relative to the signals present in the unstimulated cells. Each value represents the mean ± SE derived from four independent experiments. *$P < 0.01$ for VEGF vs. control cells. #$P < 0.01$ for TrxR1 siRNA-transfected cells vs. control siRNA-transfected cells control cells (ANOVA).

since BCNU inhibits both GR and TrxR, to gain greater insight into the roles of specific thiol-metabolizing enzymes, we designed duplex siRNA constructs to specifically knock down GR, TrxR1, and TrxR2. As shown in Figs. 2 and 6, the individual siRNA constructs targeting GR, TrxR1, or TrxR2 specifically and significantly knocked down their cognate protein targets without affecting the abundance of nontargeted proteins. siRNA-mediated knockdown of either GR, TrxR1, or TrxR2 in cultured endothelial cells markedly suppressed VEGF-induced eNOS activity and NO production (Fig. 5) and increased ROS production (Fig. 7). Each of these knockdowns inhibits eNOS activity to a similar degree, but TrxR2 knockdown yields a more pronounced increase in H_2O_2 production. Given the large number of redox-active cofactors involved in NOS catalysis, it is plausible that the knockdown of these different thiol metabolizing proteins could inhibit eNOS by distinct mechanisms, which may not all necessarily involve H_2O_2 production. As might be predicted based on its known roles of GR in glutathione redox metabolism, siRNA-mediated knockdown of GR led to a marked decrease in the GSH/GSSG in endothelial cells (Fig. 3). We were intrigued to observe that

siRNA-mediated knockdown of either TrxR1 or TrxR2 also led to a marked decrease in the GSH/GSSG to the same extent as seen following siRNA-mediated GR knockdown. This finding may reflect the cross talk between glutathione and Trx oxidoreductase systems that has been previously observed in some cell types (3). It is possible, if less likely, that siRNA-mediated TrxR knockdown directly affects the GSH/GSSG, or alternatively might alter the ratio by secondary effects as a consequence of increased ROS production.

eNOS not only produces NO but can also become "uncoupled" to produce superoxide and H_2O_2. In endothelial cells, BH4 oxidation has been shown to be associated with the production of superoxide by eNOS (4, 7, 17, 22, 24). We have recently reported that the simple depletion of endothelial BH4 (by siRNA-mediated knockdown of the key enzyme in biopterin synthesis, GTP cyclohydrolase-1) is not sufficient to promote eNOS uncoupling, but rather that it is the concentration of intracellular BH2, as well as the relative concentrations of BH4 and BH2, that together play a determining role in the redox regulation of eNOS-modulated endothelial responses (20). In the present studies, we found that siRNA-mediated
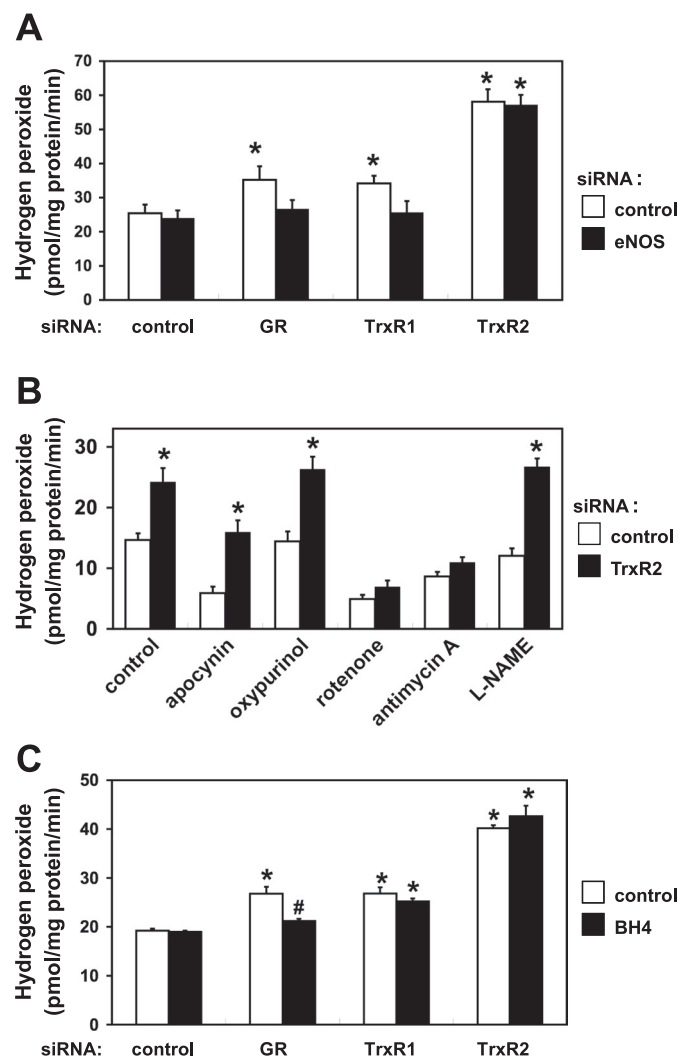
Fig. 7. H_2O_2 production from endothelial cells following knockdown of thiol-metabolizing proteins. *A*: H_2O_2 production was quantitated using the Amplex Red assay in endothelial cells transfected with various siRNA targeting constructs, as detailed in the text. *B*: BAEC were transfected with either control or TrxR2 siRNA. Forty-eight hours after transfection, BAEC were treated for 1 h with either apocynin (250 μM, NADPH oxidase inhibitor), oxypurinol (100 μM, xanthine oxidase inhibitor), rotenone (10 μM, mitochondrial complex I inhibitor), antimycin A (1 μM, mitochondrial complex III inhibitor), or N^G-nitro-L-arginine methyl ester (L-NAME; 1 mM, NO synthase inhibitor), and then assayed for H_2O_2 production. *C*: siRNA-transfected BAEC were assayed for H_2O_2 production in the presence or absence of BH4 (10 μM). Each data point represents the mean ± SE derived from four to eight independent experiments. *$P < 0.01$ compared with control siRNA-transfected cells. #$P < 0.01$ for BH4-treated vs. control cells (ANOVA).

knockdown of GR or TrxR1 (but not TrxR2) significantly decreased the intracellular BH4 concentration and also led to a decrease in the BH4-to-BH2 ratio in endothelial cells (Fig. 4). These effects on biopterin redox state are sufficient to account for the decrease in eNOS activity and the suppression of NO production (Fig. 5), as well as the increase in eNOS-derived ROS production (Fig. 7) seen following siRNA-mediated knockdown of GR or TrxR1. These findings suggest further that alterations in intracellular thiol redox state associated with oxidative stress represent a key pathway, whereby eNOS uncoupling may lead to endothelial dysfunction. Exogenous BH4 supplementation did not restore the impaired eNOS ac-

tivity that was seen after GR or TrxR1 knockdowns, despite the suppression of ROS production by BH4 supplementation following knockdown of these thiol-metabolizing proteins. We are reasonably confident that these conditions for BH4 supplementation fully restore intracellular BH4 levels, as we have shown previously for endothelial cells when cultured and treated under similar conditions (20). These observations indicate that simply restoring BH4 is not sufficient for the recovery of eNOS activity following TrxR1 knockdown, consistent with the involvement of other redox-sensitive pathways in the modulation of eNOS.

Alterations in cellular redox state following siRNA-mediated knockdown of GR, TrxR1, and TrxR2 appear to have differential effects on signaling protein phosphorylation in these cells. As shown in Fig. 6, following siRNA-mediated TrxR1 knockdown, VEGF-stimulated phosphorylation of kinase Akt or of eNOS at the stimulatory serine residue 1179 was completely blocked. By contrast, knockdown of GR or TrxR2 had a nominal effect on phosphorylation of either Akt or eNOS. VEGF-promoted dephosphorylation of eNOS at inhibitory residue Ser116 was largely unaffected by siRNA-mediated knockdowns, either of GR, TrxR1, or TrxR2 (Fig. 6). We also noted that there was a discordance between the effects on eNOS enzyme activity and phosphorylation following knockdown of these thiol-metabolizing proteins. Although much remains to be learned about the control of endothelial phosphorylation by oxidative stress, these observations indicate that there are critical differences in the redox regulation of phosphorylation pathways, depending on the specific redox pathway involved in the cellular response.

There are both qualitative and quantitative differences in the consequences of siRNA-mediated knockdown of the three different thiol disulfide oxidoreductases targeted in these studies. For example, in contrast to the increase in BH4 oxidation that was seen following siRNA-mediated knockdown of TrxR1 or GR, TrxR2 knockdown had no effect on BH4 oxidation (Fig. 4). Also, as shown in Fig. 7*A*, when the TrxR2 is knocked down, siRNA-mediated eNOS knockdown had no effect on ROS production, yet the knockdown of the TrxR1 or of GR led to a small increase in H_2O_2 production that was abrogated by eNOS knockdown. Using the Amplex Red assay to detect the extracellular production of ROS by these cells, we found no substantive change in the production of H_2O_2 following eNOS knockdown (Fig. 7). This finding provides an interesting counterpoint to our recent observation that eNOS knockdown leads to an increase in intracellular H_2O_2 production detected using a peroxide biosensor (12); these contrasting findings are consistent with previous observations that identified a discordance between the detection of intracellular and extracellular ROS using different experimental methods (16, 21). GR or TrxR1 knockdown led to a small increase in H_2O_2 production that was suppressed by BH4 supplementation (Fig. 7*C*), while the much more substantive increase in H_2O_2 production that was seen following TrxR2 knockdown was not suppressed by BH4 supplementation. The striking increase in ROS production seen following siRNA-mediated TrxR2 knockdown was not blocked by the NADPH oxidase inhibitor apocynin, nor by the xanthine oxidase inhibitor oxypurinol or NO synthase inhibitor N^G-nitro-L-arginine methyl ester (Fig. 7*B*). In contrast, the mitochondrial inhibitors rotenone (complex I inhibitor) and antimycin A (complex III inhibitor) completely suppressed the increase in H_2O_2 produc-

tion that was seen following siRNA-mediated TrxR2 knockdown (Fig. 7B). Since apocynin does not inhibit Nox4, a member of the NADPH oxidase family (19), it is still possible that Nox4 is a source of the increased H_2O_2 observed following siRNA-mediated TrxR2 knockdown. However, taken all together, these data suggest that mitochondria represent a critical source for H_2O_2 production in endothelial cells, and that the mitochondrial thiol oxidoreductase TrxR2 is a critical regulator of intracellular redox state.

Taken together, these findings indicate that the differential regulation of thiol-metabolizing proteins leads to pleiotropic effects on endothelial signaling pathways, associated with critical changes in oxidative and nitrosative stress pathways. These studies also lead us to conclude that increased ROS alters intracellular thiol redox balance, which affects eNOS activity and NO bioavailability by complex mechanisms involving the differential regulation of thiol-disulfide oxidoreductases. Greater understanding of the differential regulation of thiol-disulfide oxidoreductases may lead to the development of new pharmacological targets for disease states associated with oxidative stress in the vascular wall.

DISCLOSURES

No conflicts of interest are declared by the author(s).

REFERENCES

1. **Berndt C, Lilling CH, Holmgren A.** Thiol-based mechanisms of the thioredoxin and glutaredoxin systems: implications for diseases in the cardiovascular system. *Am J Physiol Heart Circ Physiol* 292: H1227–H1236, 2007.
2. **Cai H, Harrison DG.** Endothelial dysfunction in cardiovascular diseases: the role of oxidant stress. *Circ Res* 87: 840–844, 2000.
3. **Casagrande S, Bonetto V, Fratelli M, Gianazza E, Eberini I, Massignan T, Salmona M, Chang G, Holmgren A, Ghezzi P.** Glutathionylation of human thioredoxin: a possible crosstalk between the glutathione and thioredoxin systems. *Proc Natl Acad Sci USA* 99: 9745–9749, 2002.
4. **Crabtree MJ, Smith CL, Lam G, Goligorsky MS, Gross SS.** Ratio of 5,6,7,8-tetrahydrobiopterin to 7,8-dihydrobiopterin in endothelial cells determines glucose-elicited changes in NO vs. superoxide production by eNOS. *Am J Physiol Heart Circ Physiol* 294: H1530–H1540, 2008.
5. **Davignon J, Ganz P.** Role of endothelial dysfunction in atherosclerosis. *Circulation* 109, *Suppl* 1: III27–III32, 2004.
6. **Feletou M, Vanhoutte PM.** Endothelial dysfunction: a multifaceted disorder. *Am J Physiol Heart Circ Physiol* 291: H985–H1002, 2006.
7. **Forstermann U, Munzel T.** Endothelial nitric oxide synthase in vascular disease: from marvel to menace. *Circulation* 113: 1708–1714, 2006.
8. **Fukushima T, Nixon JC.** Analysis of reduced forms of biopterin in biological tissues and fluids. *Anal Biochem* 102: 176–188, 1980.
9. **Griffith OW.** Determination of glutathione and glutathione disulfide using glutathione reductase and 2-vinylpyridine. *Anal Biochem* 106: 207–212, 1980.
10. **Heller R, Werner-Felmayer G, Werner ER.** Antioxidants and endothelial nitric oxide synthesis. *Eur J Clin Pharmacol* 62, *Suppl* 1: 21–28, 2006.
11. **Holmgren A.** Antioxidant function of thioredoxin and glutaredoxin systems. *Antioxid Redox Signal* 2: 811–820, 2000.
12. **Jin BY, Sartoretto JL, Gladyshev VN, Michel T.** Endothelial nitric oxide synthase negatively regulates hydrogen peroxide-stimulated AMP-activated protein kinase activation in endothelial cells. *Proc Natl Acad Sci USA* 106: 17343–17348, 2009.
13. **Kou R, Michel T.** Epinephrine regulation of the endothelial nitric-oxide synthase: roles of Rac1 and beta3-adrenergic receptors in endothelial NO signaling. *J Biol Chem* 282: 32719–32729, 2007.
14. **Leopold JA, Loscalzo J.** Oxidative enzymopathies and vascular disease. *Arterioscler Thromb Vasc Biol* 25: 1332–1340, 2005.
15. **Loscalzo J.** Nitric oxide insufficiency, platelet activation, and arterial thrombosis. *Circ Res* 88: 756–762, 2001.
16. **Lubos E, Handy DE, Loscalzo J.** Role of oxidative stress and nitric oxide in atherothrombosis. *Front Biosci* 13: 5323–5344, 2008.
17. **Moen AL, Kass DA.** Tetrahydrobiopterin and cardiovascular disease. *Arterioscler Thromb Vasc Biol* 26: 2439–2444, 2006.
18. **Rinaldi M, Moroni P, Paapa MJ, Bannerman DD.** Evaluation of assays for the measurement of bovine neutrophil reactive oxygen species. *Vet Immunol Immunopathol* 115: 107–125, 2007.
19. **Serrander L, Cartier L, Bedard K, Banfi B, Lardy B, Plastre O, Sienkiewicz A, Forro L, Schlegel W, Krause KH.** NOX4 activity is determined by mRNA levels and reveals a unique pattern of ROS generation. *Biochem J* 406: 105–114, 2007.
20. **Sugiyama T, Levy BD, Michel T.** Tetrahydrobiopterin recycling, a key determinant of endothelial nitric-oxide synthase-dependent signaling pathways in cultured vascular endothelial cells. *J Biol Chem* 284: 12691–12700, 2009.
21. **Thomas SR, Witting PK, Drummond GR.** Redox control of endothelial function and dysfunction: molecular mechanisms and therapeutic opportunities. *Antioxid Redox Signal* 10: 1713–1765, 2008.
22. **Vasquez-Vivar J, Kalyanaraman B, Martasek P, Hogg N, Masters BS, Karoui H, Tordo P, Pritchard KA Jr.** Superoxide generation by endothelial nitric oxide synthase: the influence of cofactors. *Proc Natl Acad Sci USA* 95: 9220–9225, 1998.
23. **Wang J, Pan S, Berk BC.** Glutaredoxin mediates Akt and eNOS activation by flow in a glutathione reductase-dependent manner. *Arterioscler Thromb Vasc Biol* 27: 1283–1288, 2007.
24. **Wever RM, van Dam T, van Rijn HJ, de Groot F, Rabelink TJ.** Tetrahydrobiopterin regulates superoxide and nitric oxide generation by recombinant endothelial nitric oxide synthase. *Biochem Biophys Res Commun* 237: 340–344, 1997.
25. **Yamawaki H, Haendeler J, Berk BC.** Thioredoxin; a key regulator of cardiovascular homeostasis. *Circ Res* 93: 1029–1033, 2003.